The Effectiveness of Steel Beams with Extended Web-Concrete Components

Wisam Hazim Khaleel
Department of Civil Engineering, College of Engineering, University of Baghdad, Baghdad, Iraq
wissam.khalil2201D@coeng.uobaghdad.edu.iq (corresponding author)

Ahmad Jabbar Hussain Al Shimmeri
Department of Civil Engineering, College of Engineering, University of Baghdad, Baghdad, Iraq
dr.ahmadalshimmeri@coeng.uobaghdad.edu.iq

Received: 27 April 2025 | Revised: 14 May 2025 | Accepted: 30 May 2025

 DOI: https://doi.org/10.48084/etasr.11749

ABSTRACT

This study examines the structural efficacy of open web expanded asymmetric steel profile-concrete composite beams subjected to static stress. Three beam groups were investigated. The first group (solid) consisted of four specimens: the first specimen served as a reference of asymmetrical steel profiles without an extended web-composite concrete beam, while the other specimens featured expanded ratios of 30%, 50%, and 70%. The second group comprised three perforated specimens with an aperture length of 70 mm, while the third group consisted of three perforated specimens with an aperture length of 140 mm. The focus was on assessing the impact of expansion ratio, opening height, and opening length on the experimental outcomes. The findings demonstrate that augmenting the expanded ratio leads to an increase in ultimate load by about 82.25%, 113.43%, and 117.39% for the solid specimen with expanded ratios of 30%, 50%, and 70%, respectively, in comparison to the reference (unexpanded) specimen. Augmenting the expanded ratio leads to a decrease in the ultimate load by about 11.9% and 19% for specimens with tiny holes of 70 mm in length, corresponding to expanded ratios of 50% and 70%, respectively, in comparison to specimens with an expanded ratio of 30%. Augmenting the expanded ratio of perforated specimens correlates inversely with the ultimate load, as the existence of openings, particularly those of significant height, such as in the case of a 70% expanded ratio, results in a compromise of the web zone and consequently diminishes the shear resistance of the beam, alongside local buckling issues.

Keywords-composite beam; expanded ratio; asymmetrical steel profiles; sheer connectors; ductility

I. INTRODUCTION

The punched steel beams exhibit enhanced strength and rigidity due to the augmented web depth [1]. To improve the performance and strength of the steel beams in certain design situations, such as cellular, castellated, or extended beams, the web depth can be increased [2-3]. The web-opening steel beams provide several benefits over the traditional I-section building components in contemporary constructions. One of these advantages is their ability to integrate utilities, such as ducting, electrical wiring, or piping, without compromising the structural integrity of the beam, with enhanced aesthetic appeal and an increased strength-to-weight ratio. This beam type is favored in projects with extensive spans, such as stadiums, bridges, and multistory structures, due to its ability to facilitate installation and optimize space usage [3-5]. The beam's deflection rises, its shear capacity decreases, its failure modes change, and more complex design considerations become necessary when holes are punched into the steel, which weakens the beams. Compared to the regular webbed beams, the steel beams with extended webs are more costly to manufacture. Opening the steel beams also introduces residual stresses, which could affect how the beams behave structurally [6-7]. A reinforced concrete slab attached to castellated steel beams forms the composite castellated beam, which finds extensive application in building construction. To increase the load-carrying capacity and element stiffness, shear connections are utilized to guarantee that the slab and beam function in a complementary manner [8].

Under combined bending and torsion, authors in [9] studied the behavior of open web-expanded steel-concrete composite beams. Two reinforcing methods were put forward: one included just using steel stiffeners on the web sections, and the other involved subjecting the composite beams to external prestressing, while the web sections were already supported. There were two primary groups, each testing six specimens. Each group involved three specimens, labeled according to the strengthening method applied. In terms of deflection under service loads, the first strengthening method was found to lower it by 14.13% for the castellated specimens and 11.55% for the cellular specimens, whereas the second method reduced it by 147.82% and 30.11%, respectively. When steel stiffeners were applied to the castellated specimen, the torsional stiffness

increased by 27.58% concerning the twist angle. However, when these stiffeners were added to the cellular specimens, they did not seem to improve torsional performance during the early stages of loading. The second method demonstrated a more pronounced decrease in the twist angle, 93.10% for the castellated specimens and 39.53% for the cellular specimens.

Authors in [10] reported the outcomes of two concentrated load tests conducted on eight specimens of asymmetrical castellated steel beams with curved soffits, enclosed in Reactive Powder Concrete (RPC) and reinforced with lacing. The encasement of the asymmetrical castellated concave-curved soffit steel beams consists of unstiffened web components filled with RPC on each side. The lacing reinforcement's angle of inclination concerning the longitudinal axis is 45^{o}. Eight specimens with unique configurations were fabricated and tested under two substantial loads at the middle of the beam span. The results obtained from the experimental phase and the numerical analysis performed with ABAQUS indicated that an increase in the gap results in a rise in the load-deflection curve. The sample with a 122 mm gap at the support exhibited the highest load resistance against deflection compared to the reference sample without a gap and other samples with 65 mm and 105 mm gaps at the support for concavely-curved soffit steel beams.

Authors in [11] examined the performance of concrete slabs in conjunction with both symmetrical and asymmetrical castellated beams. Stud connectors serve to link the concrete slab with the steel portion. The utilization of castellated steel beams to fabricate composite steel-concrete beams is a prevalent technique in construction. Five simply supported composite beams were analyzed under two-point loading. Two specimens constructed from standard steel beams were utilized as control specimens, while three specimens were fabricated from castellated steel beams. One of these examples was constructed from a castellated steel beam with an asymmetrical cross-section, produced from two distinct standard sections (IPE120/HEA120). All composite specimens have identical dimensions and qualities for the concrete slab. The testing findings indicated that the strength and stiffness of the composite castellated steel beams were much superior to those of the composite beams constructed from the parent sections. The ultimate load capacity of a composite castellated beam constructed from an IPE120 section was 46% superior to that of a composite beam assembled from the parent beam, while the ultimate load capacity of a composite castellated beam derived from a wide-flanged HEA120 section exhibited a 21% enhancement over the parent beam control specimen. Authors in [12] investigated the flexural performance of an asymmetric castellated composite beam with an enclosed steel web, utilizing RPC casting within the steel web as a composite element, both with and without the influence of lacing rebar, by examining the gap between the two sections of the steel web. Modeling and Finite Element Analysis were conducted using ABAQUS/2016. The cross-section consists of a steel beam and a concrete deck slab, with the steel beam featuring an asymmetric configuration composed of two Tee sections; the upper segment is derived from IPE 180, while the lower section from IPE 200. RPC was utilized for the reinforcement of the steel web without welding its two sections. The results indicated an enhancement in the ultimate load capacity by utilizing gaps of 10% and 20% of the total depth, corresponding to values of 3.39 and 11.25, respectively, whereas a loss of 19.87% occurred with a gap of zero.

Authors in [13] analyzed the structural performance of 2C-cold-production castellated beams under monotonic loading till failure. Seven fabricated samples of castellated steel beams and one reference specimen were subjected to testing as supported beams under concentrated loads at two places throughout a clear span of 1730 mm. All castellated steel beams exhibited uniform characteristics and dimensions, except the width of the top and lower flanges. The effects of altering the width of the top and bottom flanges on the behavior of these beams were examined. The results demonstrated that the ratio of the ultimate load-carrying capacity of the tested castellated beams to that of the non-castellated reference beam (R_1) varied from 99.3% to 117.2%, while the ratio of the ultimate deflection of the tested beams to the same reference beam (R_1) ranged from 72.6% to 103.2%. Authors in [14] examined the behavior of castellated beams with a fiber-reinforced lightweight concrete deck slab as a modified alternative for the composite steel-concrete beams subjected to harmonic loading. The experimental program comprised six fixed-supported castellated beams measuring 2140 mm. The specimens were categorized into two groups: the first group consisted of three specimens subjected to a harmonic load effect at an operational frequency of 30 Hz for three days after which the residual strength was assessed via static load application. The second group comprised three specimens similar to those in group I, evaluated just under static load conditions. The results revealed that Lightweight Aggregate Concrete (LWAC) exerted a greater influence than Lightweight Fiber-Reinforced Aggregate Concrete (LWACF) under harmonic load conditions. The decrease in the residual strength of LWACF and Normal Weight Concrete (NWC) decks due to the harmonic load was 0.94% and 0.7%, respectively. Authors in [15] examined the experimental flexural performance of a composite concrete-reinforced asymmetrical castellated steel beam, formed by bolting two castellated hot-rolled steel channels together back-to-back, yielding a built-up I-shaped configuration with a total beam depth increase of 52.4%. Four specimens were evaluated: the first served as a reference specimen devoid of any reinforcement techniques; the second was fortified with RPC in the steel web area; and the third was enhanced with RPC reinforced by lacing rebar. All specimens were evaluated under a simply supported condition by applying two-point static loads to the concrete deck slab of the composite beams. The testing findings indicate that the ultimate load capacity rose by 24.01% and 48.34% in the second and third specimens, respectively, exhibiting enhanced stiffness, ductility, and energy absorption compared to the first specimen. Conversely, the ultimate load capacity diminished by 11.02% in the fourth specimen (reinforcement without welding in web posts), resulting in lower stiffness and ductility relative to the first specimen (controlled specimen).

Authors in [16] analyzed the behavior and responses of six double-web steel sections of non-composite and composite-reinforced concrete deck slabs, as well as castellated steel beams. The composite beams including concrete slabs and non-

composite steel beams with varying degrees of castellation were segregated from the specimens at 0%, 25%, and 50% levels. The concrete slab enhanced the ultimate load by 61.1%, 63.3%, and 55.5% for castellation ratios of 0%, 25%, and 50%, respectively. The shear strength of both non-composite and composite castellated beams diminished with an increase in the expansion ratio. The angle twist of the non-composite materials exceeded that of the composite samples owing to their superior ductility and decreased stiffness. Authors in [17] examined the structural performance of castellated steel beams with enlarged webs, highlighting the influence of design factors, including the number of apertures and cutting angle, load capacity, deflection, and stiffness. The castellated beams are designed to enhance the strength-to-weight ratio of the conventional I-beams by modifying the web into hexagonal, rectangular, or circular apertures. This design optimizes the beam load capacity and reduces weight while preserving or improving stiffness, making it ideal for long-span constructions. Seven beam specimens were tested under a single-point stress, comprising six castellated beams. The findings indicate that decreasing the number of holes enhances the load capacity and decreases deflection. The castellated beams exceeded the control sample by as much as 68.9% in the load-carrying capacity at Service Limit Deflection (SLD). The study also analyzed the impact of cutting angles (58°, 52°, and 45°) on the beam performance, determining that a 52° angle offered the optimal equilibrium between strength and stiffness.

II. EXPERIMENTAL PROGRAM

The experimental program involved fabricating, casting, and testing ten simply supported specimens (2500 mm span) of open-web expanded asymmetrical steel-concrete composite beams. The specimens consisted of hot-rolled I-sections (IPE 180 and IPE 200) and were tested under two-point monotonic loading.

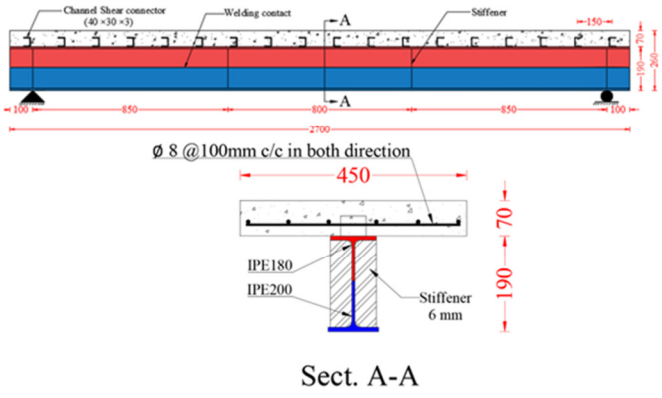

Fig. 1. Details of the BS-E0-W-L0 specimen.

The experimental work of open web expanded asymmetric steel profile composite concrete is divided into three series, based on the web expansion ratio (30%, 50%, and 70%) of the total steel depth. The specimens were divided into three main groups, the first group (solid) involved four specimens, the first specimen was a reference of asymmetrical steel profiles without an expanded web-composite concrete beam, and the others with expanded ratios of 30, 50, and 70 %. The second group involved three perforated specimens with an opening length of 70 mm, and the third group involved three perforated specimens with an opening length of 140 mm, as listed in Table I. The details of the specimens are shown in Figures 1-10.

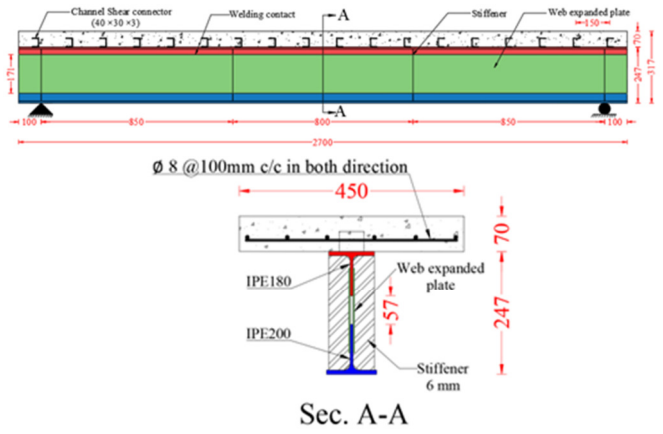

Fig. 2. Details of the BS-E30-T3-L0 specimen.

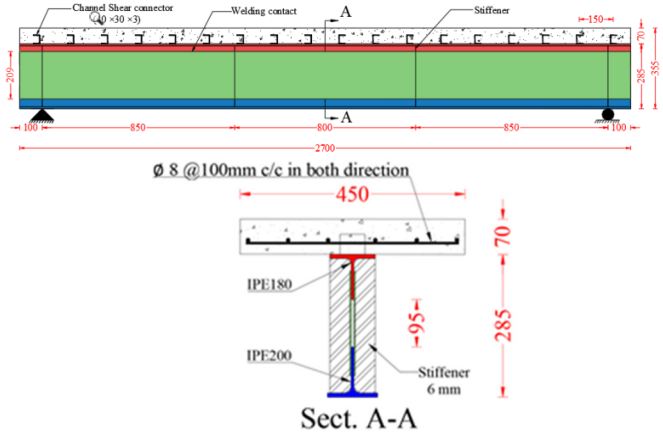

Fig. 3. Details of the BS-E50-T3-L0 specimen.

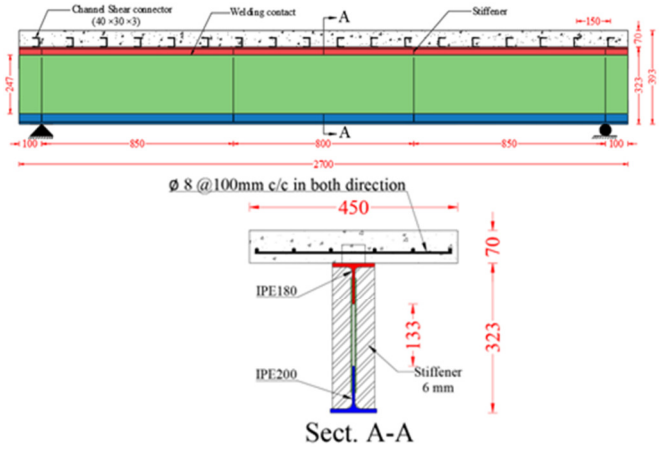

Fig. 4. Details of the BS-E70-T3-L0 specimen.

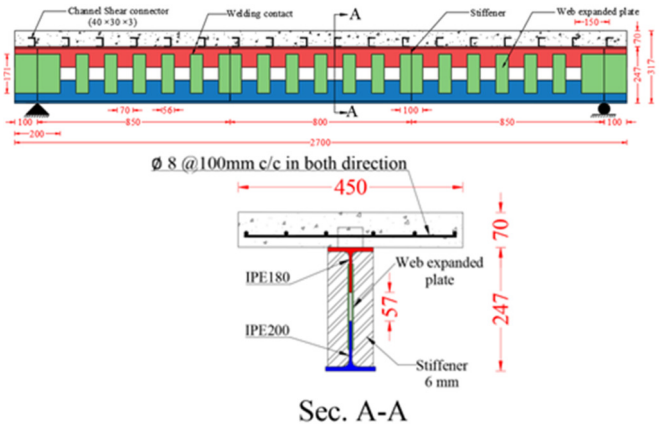

Fig. 5. Details of the BS-E30-T3-L70 specimen.

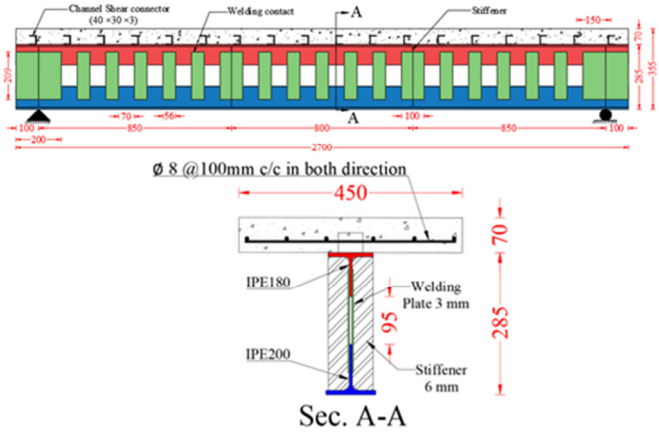

Fig. 6. Details of the BS-E50-T3-L70 specimen.

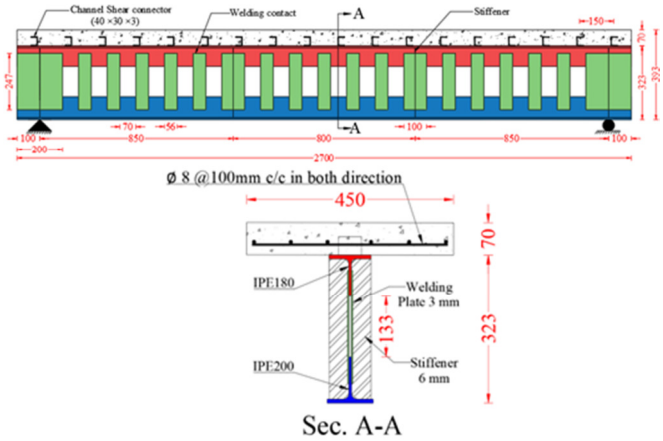

Fig. 7. Details of the BS-E70-T3-L70 specimen.

The length of the steel plates that joined between two parts of the steel tee and the length were kept constant for all specimens of 100 mm and 200 mm under point load and supports, respectively. The web post, designed to connect the two steel profile sections, was fabricated in accordance with the AISC-2016 specifications [18]. This study examined web posts with lengths of 56 mm and 140 mm.

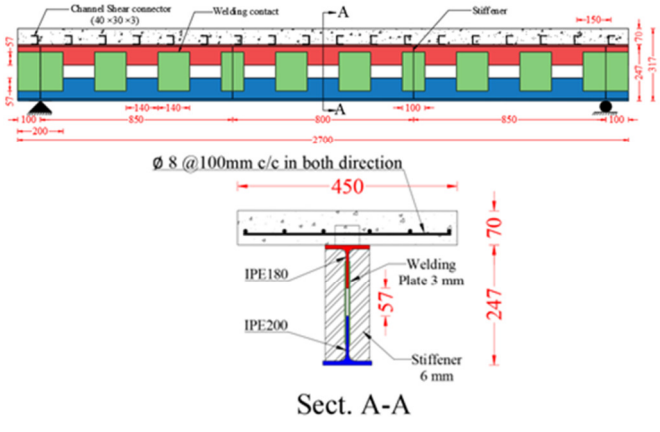

Fig. 8. Details of the BS-E30-T3-L140 specimen.

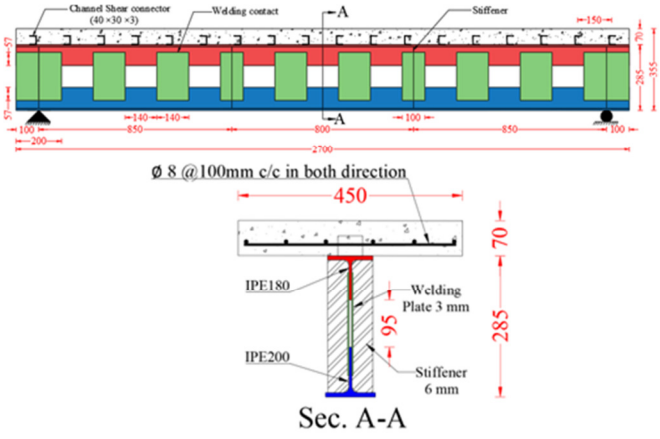

Fig. 9. Details of the BS-E50-T3-L140 specimen.

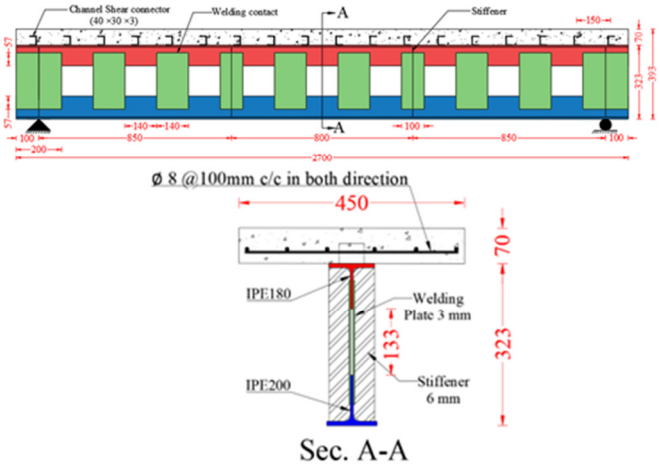

Fig. 10. Details of the BS-E70-T3-L140 specimen.

Fig. 11. Steel plate coupon samples.

Fig. 12. Testing of steel coupon.

(a)

(b)

Fig. 13. Fabrication process of specimens: (a) cutting by CNC machine, (b) reconnection by welding plate.

Fig. 14. Stiffeners and channel shear connectors.

Fig. 15. Molds and bar reinforcement of specimens.

TABLE I. TESTED BEAM DETAILS

Group	Specimen designation	Expansion ratio (%)	Web post length (mm)	Opening height (mm)	Opening length (mm)	No. of openings
G1	BS-E0-W-L0	0	NA	NA	NA	NA
	BS-E30-T3-L0	30	NA	NA	NA	NA
	BS-E50-T3-L0	50	NA	NA	NA	NA
	BS-E70-T3-L0	70	NA	NA	NA	NA
G2	BS-E30-T3-L70	30	56	57	70	18
	BS-E50-T3-L70	50	56	57	70	18
	BS-E70-T3-L70	70	56	57	70	18
G3	BS-E30-T3-L140	30	140	57	140	9
	BS-E50-T3-L140	50	140	95	140	9
	BS-E70-T3-L140	70	140	133	140	9

TABLE II. TENSILE PROPERTIES OF STEEL

Sample	Nominal thickness (mm)	Actual thickness (mm)	Yield stress (MPa)	Ultimate stress (MPa)	Elongation (%)
IPE 180 web	5.4	5.4	416.46	532.9	23.18
IPE 180 flange	8	7.5	366.59	547.42	27.82
IPE 200 web	5.6	5.6	413.39	533.14	24.85
IPE 200 flange	8.5	8	393.89	544.87	29.43
Stiffeners	6.0	5.8	379.69	443.11	26.15
Web Expanded Plates (WEP)	3.0	2.7	362.15	453.36	25.93
Shear connectors	3.0	3.0	380.98	501.42	24.30
Reinforcement bars	8 (diameter)	7.95 (diameter)	520.08	657.31	20.18

TABLE III. DETAILS OF CONCRETE MIX DESIGN PROPORTIONS

Materials			
Cement (kg/m^3)	Fine agg. (kg/m^3)	Coarse agg. (kg/m^3)	W/C ratio
422	633	1266	0.44

Table II shows the tensile properties of the steel used for fabrication, while Table III depicts the physical properties of the concrete mix proportion. Figure 11 illustrates the steel plate coupon samples, while Figure 12 displays the steel plate coupon test. Figures 13-16 present the preparation stages of the specimens. Figure 17 portrays the test setting machine of the specimens.

Fig. 16. Casting of specimens.

III. EXPERIMENTAL RESULTS

A. Properties of Hardened Concrete

Table IV shows the properties of hardened concrete. The cube compression test was conducted in accordance with BS 1881: Part 116, the cylinder compression test was performed in accordance with ASTM C 39M-17, the splitting tensile strength was measured as per ASTM C 496/C496M, and the modulus of rupture was measured as per ASTM C78.

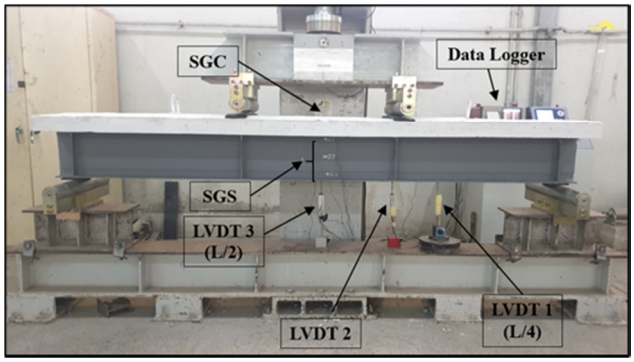

Fig. 17. Test setting machine of specimens.

TABLE IV. PROPERTIES OF HARDENED CONCRETE

Compressive strength (cubes) (MPa)	Compressive strength (cylinders) (MPa)	Splitting tensile strength (MPa)	Modulus of rupture (MPa)	Modulus of elasticity (MPa)
35.4	29.3	3.46	3.7	22001

B. Load-Midspan Deflection under Monotonic Loading

A strain gauge was fixed in the middle of the beam on the surface of the lower flange and through it, The force (P_y) corresponding to the yield strain was identified as the yielding load. Consequently, Table V displays the yield loads and the associated deflection values for all beams, as well as the ultimate loads and the associated deflection values for all beams.

For all expanded specimens, the midspan deflection at yielding exceeded that of the reference beam, where the beam of the expanded ratio of 50% and opening length of 140 mm increased by 10.2%, while the beam of the expanded ratio of 70% and without any opening increased by 54.3%, with respect to the reference beam. The mid-span deflection at the ultimate stage of the expanded beams was oscillatory when compared to the reference one. The load-deflection curves indicate that all tested beams initially exhibited linear deflection. Then, they exhibited semi-linear deflection with increasing load; however, the slope of the deflection lines was significantly reduced compared to the pre-yielding phase. The deflection curves diverged according to the extent of concrete cracking and the degree of stiffness degradation. The angle of this linear segment differed among the expanded beams. As the loads approached the ultimate value, the tested beams exhibited nonlinear deflection behavior, with the deflection curves diverging from the reference beam's deflection curve.

TABLE V. MID-SPAN DEFLECTION OF TESTED BEAMS AT DIFFERENT LOADING STAGES

Beam ID	At yielding stage			At ultimate stage	
	Load P_y (kN)	Def. Δy (mm)	% increase in Δy(%)	Load P_u (kN)	Def. Δu (mm)
BS-E0-W-L0	175	10.64	Ref.	232.2	26.48
BS-E30-T3-L0	300	11.75	10.4	423.2	28.5
BS-E50-T3-L0	400	14.49	36.2	495.6	27.55
BS-E70-T3-L0	420	16.42	54.3	504.8	25.34
BS-E30-T3-L70	255	14.26	34	298.8	25.48
BS-E50-T3-L70	240	12.2	14.7	263.2	18.69
BS-E70-T3-L70	205	11.98	12.6	242.1	26.27
BS-E30-T3-L140	270	16.1	51.3	312.7	26.34
BS-E50-T3-L140	275	11.73	10.2	300	17.42
BS-E70-T3-L140	219	11.8	10.9	257.3	19.58

1) Effect of Expanded Ratio on the Solid Specimens

The effect of the expanded ratio on the solid (without openings) specimens' load versus the mid-span deflection relationships is illustrated in Figure 18. The load-deflection curves indicate that all beams of this group, except the beam of a 70% expanded ratio, exhibit similar stiffness in the region of elasticity. However, post-yielding of the bottom flange, the beams with expanded ratios of 30% and 50% are proportional to the beam stiffness, that is, the deflection diminishes at the same load levels. The beam with the expanded ratio of 70%

gave less stiffness to the point before the ultimate stage. This may be due to the large web depth and limited thickness.

2) Effect of Expanded Ratio on the Specimens with Small Openings of 70 mm in Length

The effect of the expanded ratio on the specimens with openings of 70 mm in length load versus mid-span deflection relationships is depicted in Figure 19. The load-deflection curves indicate that all beams of this group except the beam of 70% expanded ratio exhibit similar stiffness in the region of elasticity. However, post-yielding of the bottom flange, the beams with expanded ratios of 30% and 50% are proportional to beam stiffness. The beam with an expanded ratio of 70% gave less stiffness, and this may be due to local buckling occurring in the web due to the large web depth and limited thickness.

3) Effect of Expanded Ratio on the Specimens with Large Openings of 140 mm in Length

The effect of the expanded ratio on the specimens with openings of 140 mm in length load versus the mid-span deflection relationships is portrayed in Figure 20. The load-deflection curves indicate that all beams of this group except the beam of 70% expanded ratio exhibit similar stiffness in the region of elasticity. However, post-yielding of the bottom flange, the beams with expanded ratios of 30% and 50% are proportional to the beam stiffness. The beam with a 70% expanded ratio exhibited reduced stiffness, likely attributable to local buckling in the web resulting from the substantial web depth and restricted thickness.

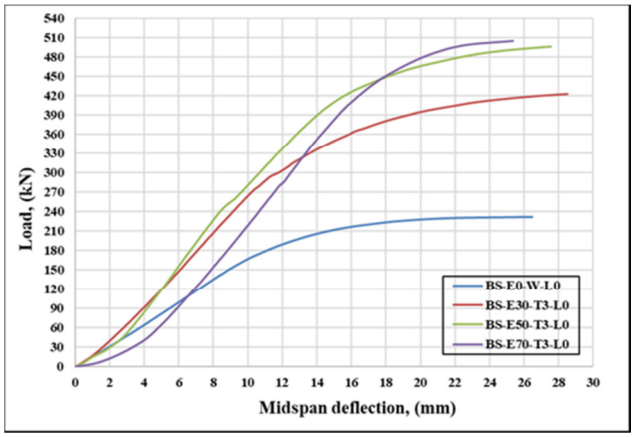

Fig. 18. Effect of expanded ratio on the load-deflection curves of the solid specimens.

4) Effect of Opening Length

Each pair of beams, which are identical in all respects except for the opening length, had a similar stiffness from the start of the loading up to approximately 80% of the ultimate load. However, as the ultimate load approached, the stiffness of the beam with the larger opening length was greater. This behavior may be attributed to the wider WEP in the 140 mm opening beam compared to the 70 mm opening beam, as shown in Figure 21.

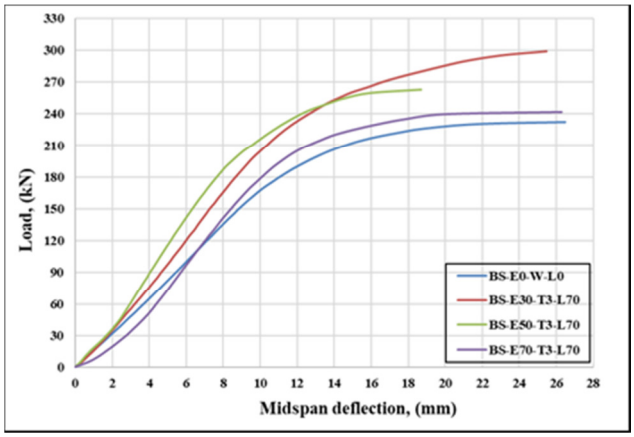

Fig. 19. Effect of expanded ratio on the load-deflection curves of the specimens with openings of 70 mm in length.

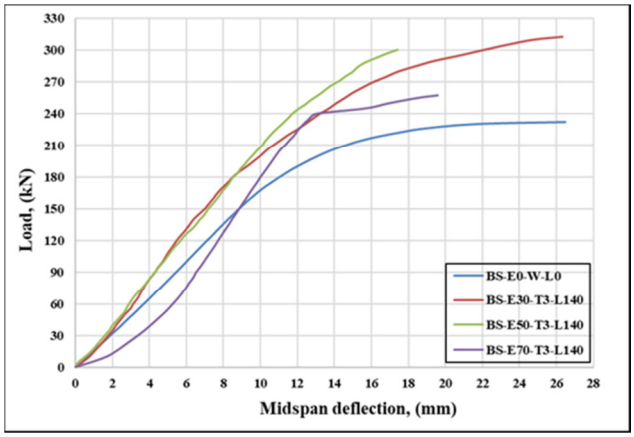

Fig. 20. Effect of expanded ratio on the load-deflection curves of the specimens with openings of 140 mm in length.

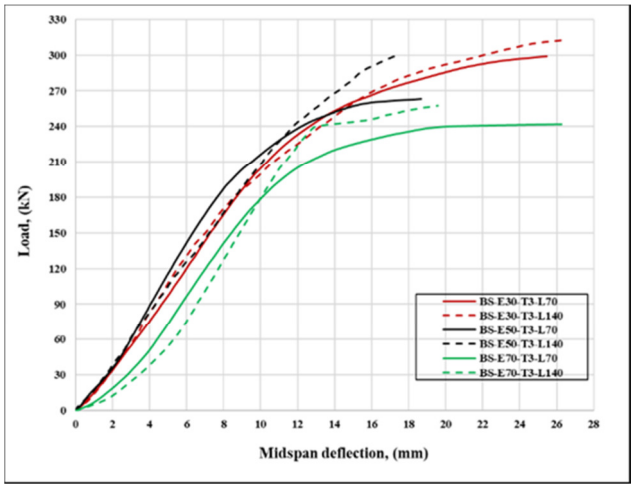

Fig. 21. Effect of opening length on the load-deflection curves.

C. Load-Carrying Capacity and Failure Mode

In the four solid specimens, made from steel beams with an expanded web ratio of 0%, 30%, 50%, and 70%, flexure failure after yielding of the bottom flange near mid-span, was observed, as illustrated in Figures 22-25. In the three perforated

specimens with an opening length of 70 mm, with an expanded web ratio of 30%, 50%, and 70%, the failure type was web expanded plate buckling (web post-buckling), while a tear in the corner of the openings was also noted, as presented in Figures 26-28. Finally, in the three perforated specimens with an opening length of 140 mm, with an expanded web ratio of 30%, 50%, and 70%, the failure type was web expanded plate buckling (web post-buckling), as shown in Figures 29-31.

Fig. 22. Mode of failure of specimen BS-E0-W-L0.

Fig. 23. Mode of failure of specimen BS-E30-T3-L0.

Fig. 24. Mode of failure of specimen BS-E50-T3-L0.

Fig. 25. Mode of failure of specimen BS-E70-T3-L0.

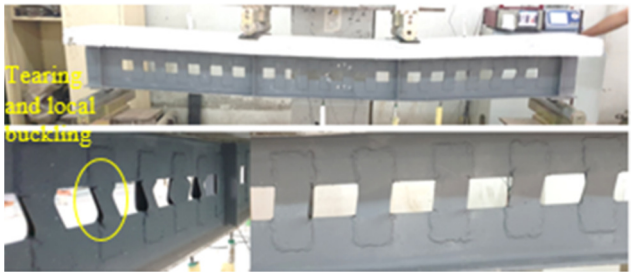

Fig. 26. Mode of failure of specimen BS-E30-T3-L70.

Fig. 27. Mode of failure of specimen BS-E50-T3-L70.

Fig. 28. Mode of failure of specimen BS-E70-T3-L70.

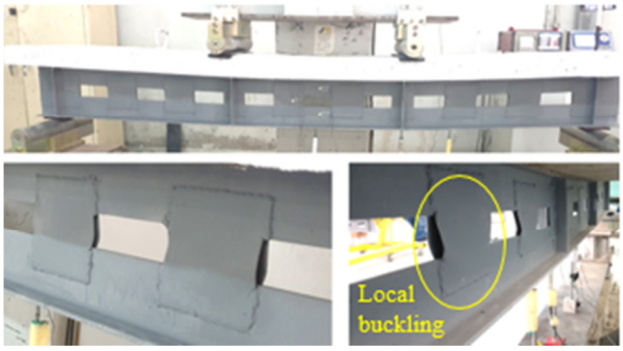

Fig. 29. Mode of failure of specimen BS-E30-T3-L140.

Fig. 30. Mode of failure of specimen BS-E50-T3-L140.

Fig. 31. Mode of failure of specimen BS-E70-T3-L140.

Table VI shows the ultimate load for all tested specimens and compares it with the failure load value of the reference one. All expanded specimens have an ultimate load greater than that of the reference (un-expanded) beam. Figure 32 demonstrates a comparison in the ultimate loads of the tested beams.

TABLE VI. ULTIMATE LOADS FOR ALL SPECIMENS

Group	Beam ID	Ultimate load (P_u) (kN)	P_u increase percentage (%)
Solid	BS-E0-W-L0	232.2	Ref.
	BS-E30-T3-L0	423.2	82.25
	BS-E50-T3-L0	495.6	113.43
	BS-E70-T3-L0	504.8	117.39
With an opening length of 70 mm	BS-E30-T3-L70	298.8	28.68
	BS-E50-T3-L70	263.2	13.35
	BS-E70-T3-L70	242.1	4.26
With an opening length of 140 mm	BS-E30-T3-L140	312.7	34.66
	BS-E50-T3-L140	300	29.19
	BS-E70-T3-L140	257.3	10.81

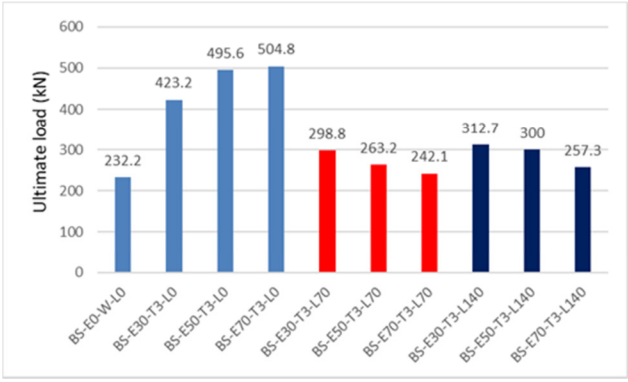

Fig. 32. A comparison in the ultimate loads of the tested beams.

1) Effect of Expanded Ratio on the Ultimate Load of the Solid Specimens

Table VI shows that increasing the expanded ratio results in an increase in the ultimate load by about 82.25%, 113.43%, and 117.39 % for the solid specimen, with an expanded ratio of 30%, 50%, and 70%, respectively, with respect to the reference (un-expanded) specimen. Increasing the expanded ratio of the solid specimens is directly proportional to the solid specimen's ultimate load.

2) Effect of Expanded Ratio on the Ultimate Load of the Specimens with Small Openings

The effect of the expanded ratio in the case of the perforated beams was different from its effect in the case of the solid beams. Although increasing the expanded ratio causes an increase in the effective depth, and thus increases the flexural strength of the beam, the presence of openings, especially those of greater height, as in the case of an expanded ratio of 70%, led to a weakening of the web zone, and thus a weakening of the shear resistance of the beam, in addition to the local buckling problems. Table VII demonstrates that increasing the expanded ratio results in a reduction in the ultimate load by about 11.9% and 19 % for the specimens with small openings of 70 mm in length, with an expanded ratio of 50% and 70%, respectively, compared with the specimen with an expanded ratio of 30%. Increasing the expanded ratio of the perforated specimens is inversely proportional to the perforated specimen's ultimate load.

TABLE VII. ULTIMATE LOAD OF THE SPECIMENS WITH SMALL OPENINGS OF 70 mm

Beam ID	Ultimate load (P_u) (kN)	P_u decrease percentage (%)
BS-E30-T3-L70	298.8	Ref.
BS-E50-T3-L70	263.2	11.9
BS-E70-T3-L70	242.1	19

3) Effect of Expanded Ratio on the Ultimate Load of the Specimens with Large Openings

Table VIII shows that increasing the expanded ratio results in a reduction in the ultimate load by about 4 and 17.7 % for the specimens with large openings of 140 mm in length, with an expanded ratio of 50% and 70%, respectively, compared to the specimen with an expanded ratio of 30%. Increasing the

expanded ratio of the perforated specimens is inversely proportional to the perforated specimen's ultimate load.

TABLE VIII. ULTIMATE LOAD OF THE SPECIMENS WITH LARGE OPENINGS OF 140 mm

Beam ID	Ultimate load (P_u) (kN)	P_u increase percentage (%)P_u (%)
BS-E30-T3-L140	312.7	Ref.
BS-E50-T3-L140	300	4.0
BS-E70-T3-L140	257.3	17.7

4) Effect of Opening Length

In the present research, two different numbers of openings were used (9 or 18) in perforated beams. Changing the number of openings while keeping the length of the weld line between the expanded web plate and the T-steel almost constant affects the ultimate load, whereas increasing the opening length (or increasing the web expanded plate length) results in an enhancement of the ultimate load. The ultimate load of the beam with an opening length of 140 mm increased by about 4.7 %, 14%, and 6.3 % for the specimen with expanded ratios of 30%, 50%, and 70%, respectively, compared to the beam with an opening length of 70 mm, as displayed in table IX.

TABLE IX. EFFECT OF OPENING LENGTH ON THE ULTIMATE LOADS

Group	Beam ID	Ultimate load (P_u) (kN)	P_u increase percentage (%)
Expanded ratio of 30%	BS-E30-T3-L70	298.8	Ref.
	BS-E30-T3-L140	312.7	4.7
Expanded ratio of 50%	BS-E50-T3-L70	263.2	Ref.
	BS-E50-T3-L140	300	14
Expanded ratio of 70%	BS-E70-T3-L70	242.1	Ref.
	BS-E70-T3-L140	257.3	6.3

D. Ductility Index

The ductility index measures a structural member's capacity to withstand substantial deformations and is equal to the ratio of mid-span deflection at failure loads to mid-span deflection at the initial yielding of the bottom flange (Table X). It is observed that all expanded beams have a ductility factor smaller than the reference unexpanded beam. The ductility factor of the expanded beams decreased by about 2.41%-40.56 % for the solid beam with an expanded ratio of 30% and the perforated beam with an expanded ratio of 50% and an opening length of 140 mm, respectively, compared to the reference beam.

TABLE X. DUCTILITY INDEX

Beam ID	Yeilding deflection (mm)	Ultimate deflection (mm)	Ductility factor (D.F.) = ultimate deflection/ yield deflection	Percentage of decrease in D.F. (%)
BS-E0-W-L0	10.637	26.484	2.49	Ref.
BS-E30-T3-L0	11.746	28.5	2.43	2.41
BS-E50-T3-L0	14.492	27.549	1.9	23.69
BS-E70-T3-L0	16.422	25.341	1.54	38.15
BS-E30-T3-L70	14.264	25.483	1.79	28.11
BS-E50-T3-L70	12.2	18.692	1.53	38.55
BS-E70-T3-L70	11.979	26.273	2.19	12.05
BS-E30-T3-L140	16.1	26.34	1.64	34.14
BS-E50-T3-L140	11.734	17.418	1.48	40.56
BS-E70-T3-L140	11.802	19.575	1.66	33.33

IV. CONCLUSION

- In all expanded samples, the mid-span deflection at the yielding stage increases relative to the reference beam; specifically, the beam with a 50% expansion ratio and a 140 mm opening exhibits a 10.2% increase, whereas the beam with a 70% expansion ratio and no openings shows a 54.3% increase compared to the reference beam.
- In the solid specimens, made from steel beams with an expanded web ratio of 0%, 30%, 50%, and 70%, flexure failure after yielding of the bottom flange near mid-span, was observed. In the perforated specimens, web post-buckling and edge tearing were noted, especially near large or closely spaced openings.
- Augmenting the expanded ratio results in an enhancement of the ultimate load by about 82.25%, 113.43%, and 117.39 % for the solid specimen with an expanded ratio of 30%, 50%, and 70%, respectively, compared to the reference (un-expanded) specimen. Increasing the expanded ratio of the solid specimen is directly proportional to the ultimate load, because an increase in the expanded ratio causes an increase in the effective depth, and thus increases the flexural resistance.
- Augmenting the expanded ratio results in a reduction in the ultimate load by about 11.9% and 19 % for the specimens with small openings of 70 mm in length, with an expanded ratio of 50% and 70%, respectively, compared to the specimens with an expanded ratio of 30%. Increasing the expanded ratio of the perforated specimens is inversely proportional to the ultimate load, because the presence of openings, especially those of high height, as in the case of an expanded ratio of 70%, led to a weakening of the web zone, and hence a weakening of the shear resistance of the beam, in addition to the local buckling problems.
- Altering the number of openings while maintaining a nearly constant weld line length between the expanded web plate and the T-steel influences the ultimate load; in specific, an increase in the opening length (or the length of the expanded web plate) leads to an augmentation of the ultimate load.

- All expanded beams have a ductility factor smaller than the reference unexpanded beam. The ductility factor of the expanded beams decreased by about 2.41%-40.56 % for the solid beam, with an expanded ratio of 30% and the perforated beam, with an expanded ratio of 50% and an opening length of 140 mm, respectively, regarding the reference beam.
- For future work, the effectiveness of steel beams with extended web-concrete components is proposed to be studied under the effect of impact load or repeated load.

REFERENCES

[1] H. W. A. Al-Thabhawee and M. A.-A. Al-Kannoon, "Improving Behavior of Castellated Beam by Adding Spacer Plat and Steel Rings," *Journal of University of Babylon for Engineering Sciences*, vol. 26, no. 4, pp. 331–344, Feb. 2018, https://doi.org/10.29196/jub.v26i4.810.

[2] Samadhan G. Morkhade and Laxmikant M. Gupta, "Behavior of Castellated Steel Beams: State of the Art Review," *Electronic Journal of Structural Engineering*, vol. 19, pp. 39–48, Dec. 2019, https://doi.org/10.56748/ejse.19234.

[3] F. Salman and A. Said, "Effect of Bridges' Width on Optimum Design of Steel Bridges," *Study of Civil Engineering and Architecture*, vol. 2, no. 3, Sep. 2013, Art. no. 77.

[4] F. De´nan, N. S. Hashim, and A. K. Mahinder Singh, "Development of efficiency analysis for I-beam steel section with web opening via numerical method," *World Journal of Engineering*, vol. 20, no. 6, pp. 1045–1056, Nov. 2023, https://doi.org/10.1108/WJE-03-2022-0117.

[5] B. F. Abdulkareem and A. F. Izzet, "Residual post fire strength of non-prismatic perforated beams," in *IOP Conference Series: Earth and Environmental Science*, Jan. 2022, vol. 961, Art. no. 012002, https://doi.org/10.1088/1755-1315/961/1/012002.

[6] S. Zhang, M. Raoof, and L. A. Wood, "Prediction of Peeling Failure of Reinforced Concrete Beams with Externally Bonded Steel Plates.," in *Proceedings of the Institution of Civil Engineers - Structures and Buildings*, vol. 110, no. 3, pp. 257–268, Aug. 1995, https://doi.org/10.1680/istbu.1995.27870.

[7] K. Geng, L. Jia, F. Xu, and Q. Li, "Experimental study on the mechanical behaviour of castellated composite beams under a negative bending moment," *Structures*, vol. 47, pp. 953–965, Jan. 2023, https://doi.org/10.1016/j.istruc.2022.11.074.

[8] R. M. Lawson, J. Lim, S. J. Hicks, and W. I. Simms, "Design of composite asymmetric cellular beams and beams with large web openings," *Journal of Constructional Steel Research*, vol. 62, no. 6, pp. 614–629, Jun. 2006, https://doi.org/10.1016/j.jcsr.2005.09.012.

[9] N. K. Oukaili and S. S. Abdullah, "Strengthening Aspects to Improve Serviceability of Open Web Expanded Steel-Concrete Composite Beams in Combined Bending and Torsion," in *IOP Conference Series: Materials Science and Engineering*, Nov. 2018, vol. 433, Art. no. 012041, https://doi.org/10.1088/1757-899X/433/1/012041.

[10] H. A. Hussein and A. J. Hussain, "Comparative Study of Structural Behavior for Asymmetrical Castellated (Concavely - Curved Soffit) Steel Beams with Different Strengthening Techniques," *Key Engineering Materials*, vol. 895, pp. 177–189, 2021.

[11] H. W. Al-Thabhawee, "Experimental investigation of composite steel–concrete beams using symmetrical and asymmetrical castellated beams," *Curved and Layered Structures*, vol. 9, no. 1, pp. 227–235, Jan. 2022, https://doi.org/10.1515/cls-2022-0019.

[12] N. K. Hussein, B. H. Al-Abbas, and A. G. A. AL-Khafaji, "Experimental and numerical behavior of composite castellated beams under repeated loads," in *the 5th International Conference on Buildings, Construction, and Environmental Engineering*, Amman, Jordan, 2024, Art. no. 020039, https://doi.org/10.1063/5.0236468.

[13] L. S. Husein and Z. A. Mohammed, "Structural behavior of composite concrete slab encasing steel castellated girder," in *The Fourth Al-Noor International Conference for Science and Technology*, Istanbul, Turkey, 2024, Art. no. 060021, https://doi.org/10.1063/5.0207395.

[14] Z. H. Dakhel and S. D. Mohammed, "Castellated Beams with Fiber-Reinforced Lightweight Concrete Deck Slab as a Modified Choice for Composite Steel-Concrete Beams Affected by Harmonic Load," *Engineering, Technology & Applied Science Research*, vol. 12, no. 4, pp. 8808–8816, 2022.

[15] N. Y. Abbas and A. J. H. Alshimmeri, "Flexural Behavior of a Composite Concrete Castellated Double Channel Steel Beams Strengthening with Reactive Powder Concrete," *Tikrit Journal of Engineering Sciences*, vol. 31, no. 2, pp. 28–42, Apr. 2024, https://doi.org/10.25130/tjes.31.2.4.

[16] F. A. Abass and A. M. Al-Khekany, "Effect of Concrete Slab on Built-up Double Web Castellated Steel Beam under Combined Flexural and Torsion Load," *Salud, Ciencia y Tecnología - Serie de Conferencias*, vol. 3, Jan. 2024, Art. no. 840, https://doi.org/10.56294/sctconf2024840.

[17] A. Naji and M. F. Kadhim, "Structural Performance of Double castellated Steel Beams with Innovative Opening Configuration," *Engineering, Technology & Applied Science Research*, vol. 15, no. 2, pp. 20616–20622, Apr. 2025, https://doi.org/10.48084/etasr.9734.

[18] S. S. Fares, S. Coulson, and D. W. Dinehart, *Castellated and Cellular Beam Design,* American Institute of steel construction, Illinois, USA, 2016.